



AMERICAN METEOROLOGICAL SOCIETY

Journal of Atmospheric and Oceanic Technology

EARLY ONLINE RELEASE

This is a preliminary PDF of the author-produced manuscript that has been peer-reviewed and accepted for publication. Since it is being posted so soon after acceptance, it has not yet been copyedited, formatted, or processed by AMS Publications. This preliminary version of the manuscript may be downloaded, distributed, and cited, but please be aware that there will be visual differences and possibly some content differences between this version and the final published version.

The DOI for this manuscript is doi: 10.1175/JTECH-D-18-0032.1

The final published version of this manuscript will replace the preliminary version at the above DOI once it is available.

If you would like to cite this EOR in a separate work, please use the following full citation:

Theocharous, E., N. Fox, I. Barker-Snook, R. Niclòs, V. Garcia Santos, P. Minnett, F. Göttsche, L. Poutier, N. Morgan, T. Nightingale, W. Wimmer, J. Høyer, K. Zhang, M. Yang, L. Guan, M. Arbelo, and C. Donlon, 2019: The 2016 CEOS infrared radiometer comparison: Part 2: Laboratory comparison of radiation thermometers.. *J. Atmos. Oceanic Technol.* doi:10.1175/JTECH-D-18-0032.1, in press.



1 **The 2016 CEOS infrared radiometer comparison: Part 2: Laboratory comparison of**
2 **radiation thermometers.**

3 **by**

4 **E. Theocharous¹, N. P. Fox¹, I. Barker-Snook¹, R. Niclòs², V. Garcia Santos², P. J.**
5 **Minnett³, F. M. Göttsche⁴, L. Poutier⁵, N. Morgan⁶, T. Nightingale⁷, W. Wimmer⁸, J.**
6 **Høyer⁹, K. Zhang¹⁰, M. Yang¹⁰, L. Guan¹⁰, M. Arbelo¹¹, C. J. Donlon¹²**

7 ¹ NPL, Hampton Road, Teddington, TW11 0LW, UK.

8 ² Faculty of Physics, University of Valencia, Dr. Moliner, 50, 46100 Burjassot, Spain.

9 ³ Rosenstiel School, University of Miami, 4600 Rickenbacker Causeway, Miami, FL 33149,
10 USA.

11 ⁴ IMK-ASF, Karlsruhe Institute of Technology (KIT), Hermann-von-Helmholtz-Platz 1,
12 76344 Eggenstein-Leopoldshafen, Germany.

13 ⁵ ONERA, 2, avenue Edouard Belin, 31055 Toulouse Cedex4, France.

14 ⁶ CSIRO Oceans and Atmosphere, Castray Esplanade, Hobart 7000, Australia.

15 ⁷ STFC Rutherford Appleton Laboratory, Chilton, Didcot, Oxon OX11 0QX, UK.

16 ⁸ Southampton University, European Way, Southampton, SO14 3ZH, UK.

17 ⁹ Danish Meteorological Institute (DMI), Centre for Ocean and Ice, Lyngbyvej 100, 2100
18 København Denmark.

19 ¹⁰ Ocean University of China, 238 Songling Road, Qingdao, 266100, China.

20 ¹¹ Grupo de Observacion de la Tierra y la Atmosfera (GOTA), ULL, Spain.

21 ¹² European Space Agency, Keplerlaan 1, 2201 AZ, Noordwijk, The Netherlands

22 *Corresponding author address:* E. Theocharous, Environmental Climate and Optical Group,
23 NPL, Hampton Road, Teddington TW11 0LW, UK.
24 E-mail: e.theo@npl.co.uk

25

26 **Abstract**

27 To ensure confidence, measurements carried out by imaging radiometers mounted on satellites
28 require robust validation using ‘fiducial quality’ measurements of the same ‘in-situ’ parameter.
29 For surface temperature measurements this is optimally carried out by radiometers measuring
30 radiation emitted in the infrared region of the spectrum, co-located to that of a satellite
31 overpass. For ocean surface temperatures the radiometers are usually on-board ships to sample
32 large areas but for Land and Ice they are typically deployed at defined geographical sites. It is
33 of course critical that the validation measurements and associated instrumentation are
34 internationally consistent and traceable to international standards. The Committee on Earth
35 Observation Satellites (CEOS) facilitates this process and over the last two decades has
36 organised a series of comparisons, initially to develop and share best practise, but now to assess
37 metrological uncertainties and degree of consistency of all the participants. The fourth CEOS
38 comparison of validation instrumentation: blackbodies and infrared radiometers, was held at
39 the National Physical Laboratory (NPL) during June and July 2016 sponsored by the European
40 Space Agency (ESA). The 2016 campaign was completed over a period of three weeks and
41 included not only laboratory based measurements but also representative measurements carried
42 out in field conditions, over land and water. This paper is one of a series and reports the results
43 obtained when radiometers participating in this comparison were used to measure the radiance
44 temperature of the NPL ammonia heat-pipe blackbody during the 2016 comparison activities
45 i.e. an assessment of radiometer performance compared to international standards. This

46 comparison showed that the differences between the participating radiometer readings and the
47 corresponding temperature of the reference blackbody were within the uncertainty of the
48 measurements but there were a few exception, particularly for a reference blackbody
49 temperature of -30 °C. Reasons which give rise to the discrepancies observed at the low
50 blackbody temperatures were identified.

51

52 **1 INTRODUCTION**

53

54 The measurement of the Earth's surface temperature and, more fundamentally, its temporal
55 and spatial variation, is a critical operational product for meteorology and an essential
56 parameter for climate monitoring (Yoder et al., 2014). Satellites have been monitoring global
57 surface temperature for some time. However, it is essential for long-term records that such
58 measurements are fully anchored to international physical standards as represented by the
59 Systeme International (SI) units. Field-deployed infrared radiometers¹ currently provide the
60 most accurate measurements of the Sea Surface Temperature and are currently used for
61 calibration and validation of Earth observation radiometers (Minnett and Corlett, 2012). These
62 radiometers are in principle calibrated traceably to SI units, generally through a blackbody
63 radiator. However, they are of varying design and are operated by different teams in different
64 parts of the globe, and the quality of the blackbody radiator can be variable. It is essential for
65 the integrity of their use, that any differences in their measurements are understood, so that any
66 potential biases are removed and are not transferred to satellite sensors (Minnett et al., 2002).
67 One way of ensuring this is for the radiometers to be calibrated against a common high quality

1 This report describes the comparison of instruments which are referred to by participants as "radiometers". However, radiometers generally measure and report radiometric parameters in radiometric units (W, Wm⁻², etc.). The instruments dealt with here measure temperature (in units of degrees C or K) so they are thermometers or "radiation thermometers". However, in view of the common usage of the terminology for this application, this report will continue to use the term "radiometer".

68 SI traceable blackbody and be tested alongside each other under field conditions. As part of
69 this process, it is also essential that each radiometer and its procedure for use is well-
70 documented and a detailed uncertainty budget related to the traceability of its measurements to
71 SI units is created. To recognise this rigour and distinguish such measurements from other ‘in-
72 situ’ measurements the term ‘fiducial reference measurements’ (FRM) has been established
73 (<https://earth.esa.int/web/sppa/activities/frm>) and is being used for similar measurements of
74 other Earth Observation parameters e.g. Ocean colour, Sea height etc.

75 Previous CEOS comparisons of terrestrial based infrared (IR) radiometric instrumentation used
76 to support calibration and validation of satellite borne sensors, with emphasis on sea/water
77 surface temperature, were completed in Miami (Florida, USA) in 2001 (Barton et al., 2004)
78 (Rice et al., 2004) and at the National Physical Laboratory (NPL) and Miami (Florida, USA)
79 in 2009 (Theocharous and Fox, 2010) (Theocharous et al., 2010). However, seven years had
80 passed, and many of the satellite sensors originally underpinned were at best nearing the end
81 of their life. Under the auspices of the Committee of Earth Observation Satellites (CEOS), the
82 European Space Agency (ESA) established a new comparison of terrestrial based Infra Red
83 (IR) radiometric instrumentation, in this case with their use expanded to support calibration
84 and validation of satellite borne sensors for sea/water/land/ice surface temperature, this was
85 completed at NPL during June and July 2016. The expansion of applications reflected the
86 capabilities of new sensors such as the Sea and Land Surface Temperature Radiometer
87 (SLSTR) on the Copernicus Sentinel 3 satellite and the increasing importance of Land and Ice
88 temperature measurements, particularly for climate monitoring. The objectives of the 2016
89 comparison were to establish the “degree of equivalence” between terrestrially based IR
90 Calibration/Validation (Cal/Val) measurements made in support of satellite observations of the
91 Earth’s surface temperature and to ensure their traceability to SI units through the participation
92 of National Metrology Institutes (NMIs). The comparison was organised through an ESA

93 project called Fiducial Reference Measurements for Surface Temperatures derived by Satellite
94 ([FRM4STS](http://www.FRM4STS.org)) which also carried out a critical review of community measurement practises,
95 details can be found at <http://www.FRM4STS.org> .

96 During the 2016 comparison, NPL acted as the pilot laboratory and provided traceability to SI
97 units during laboratory comparisons. Stage 1 consisted of Lab comparisons, and took place at
98 NPL during the week starting on 20th June 2016. This Stage involved laboratory measurements
99 of participants' blackbodies calibrated using the NPL Absolute Measurement of a Blackbody
100 Emitted Radiance (AMBER) reference transfer radiometer (Theocharous et al., 1998) and the
101 Physikalisch-Technische Bundesanstalt (PTB) infrared radiometer. In another exercise run
102 concurrently, participants' radiometers were calibrated using the NPL ammonia heat-pipe
103 reference blackbody (Chu and Machin, 1999). Stage 2 took place at Wraysbury reservoir
104 (Spelthorne, TW19 5NX, UK) during the week starting on 27th June 2016 and involved field
105 measurements of the temperature of the surface of the water. Stage 2 included the testing of
106 the same radiometers alongside each other, completing direct daytime and night-time
107 measurements of the surface temperature of the water. Stage 3 took place in the grounds of
108 NPL during the week starting on 4th July 2016 and involved field measurements of the
109 temperature of the surface of a number of solid targets. Stage 3 included the testing of the same
110 radiometers alongside each other, completing direct daytime and night-time measurements of
111 the surface temperature of short grass, clover, soil, sand, gravel and tarmac/asphalt.

112 This paper provides the results of the comparison of the participants' radiometers while they
113 were viewing the NPL ammonia heat-pipe reference blackbody. All measurements reported by
114 the participants, along with their associated uncertainties, were analysed by the pilot laboratory
115 and are presented in this report.

116 The findings described in this paper are important because they confirm performance of the
117 radiometers which participated in the comparison. This is a critical requirement because these
118 radiometers are used to validate the surface temperature measurements provided by imaging
119 radiometers mounted on satellites.

120 Section 2 of this paper summarises the organisation of the radiometer comparison, while
121 Section 3 provides the measurement procedure which was employed during this comparison.
122 Section 4 describes the characteristics of the radiometers which took part in the comparison
123 while Section 5 compares and discusses the findings of the comparison.

124

125 **2 ORGANISATION OF THE COMPARISON**

126

127 Recognising the increasing reliance of satellite operators and their customers/users on the
128 quality of the data that comes from the satellite sensors it is essential that measurements used
129 for their validation can be relied upon over a wide range of operational environments.
130 Investments in projects which support the long term delivery of data for decades to come, such
131 as the European Union (EU) Copernicus program, have encouraged the community to subject
132 such measurements to the scrutiny and practises common to other sectors of commerce i.e.
133 comparison and/or audit by independent experts. The international metrology community has
134 a responsibility to support such initiatives and therefore undertake regular comparisons
135 between themselves of key quantities and report the results in open literature to ensure global
136 consistency and transparency to the SI (<https://kcdb.bipm.org/>). To support this process, they
137 have established procedures and guidance on how to optimally carry out such comparisons and
138 analyse the results. The Earth Observation (EO) community is taking advantage of this
139 knowledge and adopting the guidance to meet its needs. The Quality Assurance Framework

140 for Earth Observation (QA4EO) [<http://qa4eo.org/>] developed by CEOS is the embodiment of
141 this, and the comparison described below was organised following these metrology-based
142 guidelines and practises.

143 This meant that before the comparison took place, a formal protocol describing the nature of
144 the comparison, timelines, measurements to be undertaken, reporting format and, in particular,
145 guidance on the content and presentation of an uncertainty budget was developed and agreed
146 by all participants. Such protocols can then be subsequently used, with minor modifications,
147 for similar comparisons in the future and will ensure a degree of consistency in how to interpret
148 results.

149 During the 2016 comparison, NPL acted as the pilot laboratory and, with the aid of PTB,
150 provided formal traceability to SI units during the laboratory comparisons at NPL. NPL was
151 supported with specialist application advice from University of Southampton, Rutherford and
152 Appleton Lab (RAL) and Karlsruhe Institute of Technology (KIT) during the development of
153 the necessary protocols.

154 This report provides the results, together with uncertainties as provided by the participants, of
155 the radiometer measurements of the NPL ammonia heat-pipe blackbody operating at seven
156 fixed temperatures as performed in one of NPL's temperature-controlled laboratories during
157 the week beginning 20th June 2016. The laboratory comparison of the participants' blackbodies,
158 as measured by the NPL AMBER radiometer and the PTB infrared radiometer, as well as the
159 Water Surface Temperature (WST) comparison at Wraysbury reservoir and the Land Surface
160 Temperature (LST) comparison that took place in the NPL grounds are being presented
161 elsewhere.

162 During the 2016 comparison, all participants were encouraged to develop uncertainty budgets
163 for all measurements they reported. In order to achieve optimum comparability, tables

164 containing the principal influence parameters for the measurements were provided to all
165 participants, highlighting the importance of including in their uncertainty budgets uncertainty
166 contributions due to the primary calibration of the radiometer, the linearity of response of the
167 radiometer, drift since the last calibration, effects due to ambient temperature fluctuations,
168 atmospheric absorption/emission, as well as the repeatability and reproducibility of their
169 measurements. All measurements reported by the participants, along with their associated
170 uncertainties, were analysed by the pilot laboratory, blind to all participants, and are presented
171 in this report.

172

173 **3 MEASUREMENT PROCEDURE FOR THE RADIOMETER LAB COMPARISON**

174

175 The NPL ammonia heat-pipe reference blackbody (Chu and Machin, 1999) was used in the
176 comparison of the participating radiometers. A schematic of this blackbody is shown in
177 Figure 1. This blackbody uses a heat-pipe to control the blackbody cavity temperature which
178 results in negligible temperature gradients along the length of the cavity. The length of the
179 ammonia heat-pipe blackbody cavity is 300 mm, and it has a 75 mm internal diameter with a
180 120° cone angle at the end wall. The blackbody cavity is coated with a high-emissivity Nextel
181 black paint. The emissivity of the blackbody cavity has been calculated using the series integral
182 method (Berry, 1981). The effective emissivity of the cavity was estimated to be 0.9993,
183 assuming an emissivity of 0.96 for the Nextel black coating (Betts, *et al.*, 1985).

184 The temperature of the blackbody cavity was obtained from an ITS-90 calibrated Platinum
185 Resistance Thermometer (PRT) which was inserted into a well of 150 mm depth in the rear of
186 the cavity. The front of the blackbody contained a circular support which allowed aperture
187 plates with different diameters to be positioned in front of the blackbody cavity. The blackbody

188 had a 75 mm diameter aperture mounted on the blackbody casing. There was a total distance
189 of approximately 75 mm from the front of this aperture to the actual blackbody cavity. This, in
190 turn, meant that if radiometers with a large field of view were measuring the reference
191 blackbody, then there was a possibility that they could be seeing parts which were outside of
192 the blackbody cavity, even when they were placed right up against the front of the blackbody
193 casing. While participants were free to position and align their blackbodies at any position in
194 front of the reference blackbody, most of the participants placed their radiometers right up
195 against the reference blackbody, in order to ensure that the blackbody cavity overfilled the
196 entire Field of View of their radiometers.

197 The temperature of the blackbody cavity was controlled by a cylindrical heat exchanger which
198 fitted closely around the blackbody cavity. Heat transfer fluid was circulated through a
199 continuous 6 mm wide helical groove which was machined in the surface of the internal
200 cylinder. Full information on the ammonia heat-pipe blackbody can be found elsewhere (Chu
201 and Machin, 1999).

202 At sub-ambient temperatures i.e. at temperatures below the Dew point, the blackbody cavity
203 was purged with dry nitrogen, in order to prevent water from condensing on the internal
204 surfaces of the cavity which could damage the internal black coating and change the effective
205 emissivity. The dry nitrogen gas was fed into the blackbody cavity from the rear. Its
206 temperature was iso-thermalised within the feed tube which was embedded within the wall of
207 the heat pipe. The gas was introduced into the front of the blackbody cavity via a gas
208 distribution ring consisting of 12 holes of 1.5 mm diameter. In order to reduce the effect of
209 convection currents from the surroundings, the aperture of the blackbody cavity was open
210 whilst measurements were being made but was blocked at all other times with an insulation
211 plug.

212 For each comparison point, the reference blackbody was set at a nominal temperature known
213 only to NPL and enough time was allowed for its cavity temperature to stabilise to the new
214 setting. Once the operating temperature had been selected, the system required just 30 minutes
215 to reach temperatures greater than 0 °C, but as much as 3 hours to reach temperatures on the
216 region of -30 °C. Once the set-point had been reached, the blackbody required another 0.5 to
217 1 hour to stabilize at the new temperature.

218 Once the temperature of the reference blackbody was stabilised at a particular temperature,
219 each participant was allowed a maximum period of 30 minutes to position their radiometer,
220 align it to the aperture of the blackbody and take measurements at that particular temperature
221 setting. The order with which radiometers completed the measurements at the beginning of the
222 comparison depended on the readiness of the radiometers of the different participants to do
223 measurements at that particular time. Towards the end of the comparison, participants were
224 allocated 30 minute periods, according to timetables which were circulated to all participants.
225 Participants with more than one radiometer were asked to arrange for the 30 minute
226 measurement period to be shared between all their measuring radiometers. Figure 2 shows the
227 Rosenstiel School of Marine and Atmospheric Sciences (RSMAS) M-AERI radiometer
228 viewing the ammonia heat-pipe blackbody during the comparison.

229 The temperature of the reference blackbody was continuously logged referenced to Universal
230 Time Coordinated (UTC) and the participants were asked to use the same time reference. This
231 allowed the direct comparison of the measurements of each participant with the corresponding
232 measurements of the reference blackbody.

233 Participants were asked to provide their measurements in pre-defined spreadsheets. The top of
234 each spreadsheet indicated the date on which the measurements shown in the spreadsheet were
235 performed. Each spreadsheet consisted of a minimum of three columns. The first column

236 indicated the time of the measurement, in a UTC format. The second column gave the
237 brightness temperature of the reference blackbody, as measured by the participant, at the time
238 indicated in the first column. The third column provided the combined standard uncertainty of
239 the measurement of the brightness temperature estimated by the participant corresponding to
240 the measurement indicated in the second column.

241 Participants were encouraged to develop and provide full uncertainty budgets for their
242 measurements. In order to help participants to do this, tables were provided listing the
243 parameters which were likely to contribute to the uncertainty of the measurement. Some
244 participants provided completed tables, providing extensive information on each uncertainty
245 contribution, while other participants provided considerably less information on their
246 uncertainty budgets, and this is recognised by the community as an area where more work is
247 needed. Full information on the uncertainty budgets provided by participants can be found
248 elsewhere (Barker Snook, et al., 2017).

249 The measurements were carried out in a lab whose temperature was controlled to ± 1 °C around
250 20 °C and the humidity was controlled to $\pm 5\%$ around 45 % during these measurements.

251

252 **4 PARTICIPANTS' RADIOMETERS AND MEASUREMENTS**

253

254 A total of 19 radiometers operating on 24 different measurement channels took part in the 2016
255 radiometer lab comparison. This section gives brief descriptions of the participating
256 radiometers. A summary of the most important parameters of the participating radiometers is
257 given in Table 1.

258

259 The University of Valencia CIMEL Electronique CE312-2 radiometers

260 Two radiometers were provided by the Dept. of Earth Physics and Thermodynamics of the
261 University of Valencia, Spain. Both radiometers were of the CIMEL Electronique CE312-2
262 type and operated in six spectral bands, 8.0 μm to 13.3 μm , 10.9 μm to 11.7 μm , 10.2 μm to
263 11.0 μm , 9.0 μm to 9.3 μm , 8.5 μm to 8.9 μm , and 8.3 μm to 8.6 μm . These radiometers were
264 able to provide measurements of the brightness temperature of the reference blackbody for
265 each of the six bands on which they were able to operate. Both radiometers employed
266 germanium windows and used narrow band filters with zinc sulphide substrates to select the
267 different wavelength bands. Both instruments had a 10 degree full angle Field of View and
268 included a built-in radiance reference made of a concealable gold-coated mirror which enabled
269 comparison between the target radiance and the reference radiation from inside the detector
270 cavity. The temperature of the detector was measured with a calibrated PRT, thus allowing
271 compensation for the cavity radiation. The relevant outputs of the radiometer were the detector
272 temperature and the difference in digital counts between the signals from the target and the
273 detector cavity. The quoted uncertainty of measurements made by the first radiometer (Unit 1)
274 was 370 mK, while the corresponding value for the second radiometer (Unit 2) was 360 mK
275 (Barker-Snook et al., 2017). Further information on these radiometers can be found in Sicard
276 et al., (1999) and in Legrand et al., (2000).

277

278 The KIT Heitronics KT15.85 IIP radiometer

279 The radiometer provided by the Institute of Meteorology and Climate Research - Atmospheric
280 Trace Gases and Remote Sensing (IMK-ASF), Karlsruhe Institute of Technology (KIT),
281 Germany was a Heitronics KT15.85 IIP radiometer with L6 lens
282 (https://www.heitronics.com/fileadmin/content/Prospekte/KT15IIP_e_V510.pdf). This was a
283 single channel radiometer based on a pyroelectric infrared detector. This type of sensor links

284 radiance measurements via beam-chopping to internal reference temperature measurements
285 and thermal drift can practically be eliminated. The field of view of this radiometer was 8.3°
286 (full angle). The KT15.85 IIP responded in the 9.6 μm to 11.5 μm spectral range, had a quoted
287 uncertainty of approximately 0.3 K (Barker Snook, et al., 2017, page 29) over the temperature
288 range relevant to land surfaces and claimed good long-term stability.

289

290 The ONERA radiometers

291 Four radiometers were provided by the Office National d'Etudes et de Recherches
292 Aérospatiales (ONERA), France. The first three radiometers were Heitronics KT19.85 II
293 (https://www.heitronics.com/fileadmin/content/Prospekte/KT15IIP_e_V510.pdf) which had a
294 95 mm target diameter when viewing a target at a distance of 2 m. These radiometers operated
295 in the 9.6 μm to 11.5 μm spectral band and offered a 60 mK temperature resolution. Their
296 quoted measurement uncertainty was ± 0.5 °C + 0.7 % of the difference between target and
297 housing temperature. The fourth ONERA radiometer was a BOMEM MR304SC
298 Spectroradiometer
299 ([https://library.e.abb.com/public/654dfb800019d7168525712d00693379/4314%20MR304SC
300 %20Spec.pdf](https://library.e.abb.com/public/654dfb800019d7168525712d00693379/4314%20MR304SC%20Spec.pdf)) covering the 3 μm to 13 μm wavelength range with two detectors, one InSb and
301 one MCT detector, with a 4 cm⁻¹ resolution. This radiometer had a 20° (full angle) FoV. The
302 measured radiance spectrum was converted into brightness temperature and averaged over the
303 9.6 μm to 11.5 μm wavelength range of the Heitronics radiometers. The temperature
304 uncertainty was quoted for each measurement and ranged from 0.2 K to 0.4 K, depending on
305 the blackbody set temperature (Barker-Snook et al., 2017).

306

307 The CSIRO Infrared Sea surface temperature Autonomous Radiometer (ISAR)

308 The radiometer provided by the Marine National Facility, Commonwealth Scientific and
309 Industrial Research Organisation (CSIRO), Australia was an ISAR 5D radiometer. This
310 radiometer had a Field of View of 7 degrees (full angle) and responded to wavelengths in the
311 9.6 μm to 11.5 μm spectral band. This radiometer offered a 10 mK temperature resolution. The
312 measurement uncertainty was quoted for each blackbody temperature measured and ranged
313 from 85 mK at -30 $^{\circ}\text{C}$ to 57 mK at 45 $^{\circ}\text{C}$. Full information on this type of radiometer is given
314 by Donlon et al., (2008) and Wimmer and Robinson, (2016).

315

316 The STFC RAL SISTeR radiometer

317 The radiometer provided by the Science and Technology Facilities Council Rutherford
318 Appleton Laboratory, UK, was the Scanning Infrared Sea Surface Temperature Radiometer
319 (SISTeR). SISTeR was a chopped, self-calibrating filter radiometer manufactured by RAL
320 Space. It had a single-element Deuterated Lanthanum Alanine-doped TriGlycine Sulphate
321 (DLATGS) pyroelectric detector, a filter wheel containing up to six band-defining filters and
322 two internal reference blackbodies, one operating at ambient temperature and the other heated
323 to approximately 17 K above ambient. During operation, the radiometer selected (with a scan
324 mirror) successive views of each of the blackbodies and the external scene in a repeated
325 sequence. For Sea Surface Temperature (SST) measurements, the external measurements
326 included views of the sea surface and the sky at the complementary angle. The instrument field
327 of view was approximately 13 $^{\circ}$ (full angle). During this comparison, a filter centred at 10.8 μm
328 was used. The measurement uncertainty was quoted for each blackbody temperature measured
329 and ranged from 128 mK at -30 $^{\circ}\text{C}$ to 19 mK at 45 $^{\circ}\text{C}$. Further information on the SISTeR
330 radiometer can be found in <http://www.stfc.ac.uk/research/environment/sister/>

331

332 The Southampton University ISAR radiometer

333 The radiometer provided by the National Oceanography Centre of Southampton University,
334 UK, was an ISAR-5D with a Field of View of 7 degrees (full angle). The radiometer responded
335 to wavelengths in the 9.6 μm to 11.5 μm spectral band. This radiometer offered a 10 mK
336 temperature resolution. The measurement uncertainty was quoted for each blackbody
337 temperature measured and ranged from 120 mK at -30 °C to 60 mK at 30 °C. Full information
338 on the ISAR radiometer can be found in the papers by Donlon et al., (2008) and Wimmer and
339 Robinson, (2016).

340

341 The DMI radiometers

342 Two radiometers were provided by the Danish Meteorological Institute (DMI), Denmark. The
343 first radiometer was an ISAR-5D. The measurement uncertainty of this radiometer was quoted
344 for each blackbody temperature measured and ranged from 83 mK at -15 °C to 59 mK at 45
345 °C. Full information on this radiometer can be found in the paper by Donlon et al., (2008) and
346 in the sections dealing with the CSIRO and Southampton University radiometers. The second
347 radiometer was a Campbell Scientific IR120. This was a broadband radiometer measuring over
348 the 8 μm to 14 μm wavelength range. This radiometer offered a 10 mK temperature resolution
349 and a quoted measurement uncertainty of 200 mK. For further information on the Campbell
350 Scientific IR120 radiometer see:

351 https://s.campbellsci.com/documents/eu/manuals/ir100_ir120.pdf

352

353 The OUC, Qingdao radiometers

354 Two radiometers were provided by the Ocean University of China (OUC), Qingdao, China.
355 The first radiometer was an ISAR 5C radiometer. This radiometer had a Field of View of 7
356 degrees (full angle) and responded to wavelengths in the 9.6 μm to 11.5 μm spectral band. This
357 radiometer offered a 10 mK temperature resolution and a quoted measurement uncertainty of
358 100 mK for all blackbody temperatures measured. Full information on this radiometer can be
359 found in Donlon et al., (2008) and in Wimmer and Robinson, (2016).

360 The second radiometer provided by the OUC was an Ocean University of China First Infrared
361 Radiometer (OUCFIRST) developed for measurements of the sea surface temperature. The
362 OUCFIRST radiometer was similar to the ISAR radiometer and was based on the Heitronics
363 KT15.85 IIP detector which responds in the 9.6 μm to 11.5 μm wavelength range. The
364 OUCFIRST radiometer also included two internal reference blackbody sources. This
365 radiometer was calibrated before and after each measurement campaign using an external
366 blackbody. The quoted measurement uncertainty of this radiometer was 100 mK for all
367 blackbody temperatures measured.

368

369 The GOTA CIMEL Electronique CE312-2 radiometer

370 The radiometer provided by Grupo de Observacion de la Tierra y la Atmosfera (GOTA)
371 Universidad de La Laguna, Spain was a CIMEL Electronique CE312-2 radiometer. This
372 radiometer incorporated a thermopile detector and was able to operate over six wavelength
373 bands spread over the 8 μm to 13 μm wavelength range. The measurement uncertainty of this
374 radiometer was quoted for each blackbody temperature measured and ranged from 400 mK to
375 500 mK for all measurements completed by this radiometer. Further information on this

376 radiometer can be found in Sicard et al., (1999) and Legrand et al., (2000) as well as in the
377 section dealing with the University of Valencia radiometers.

378

379 The RSMAS M-AERI radiometer

380 The radiometer provided by the Rosenstiel School of Marine and Atmospheric Science
381 (RSMAS), University of Miami, USA was a Marine-Atmospheric Emitted Radiance
382 Interferometer (M-AERI) Mk-3. This radiometer, like its predecessors, was based on a Fourier-
383 Transform Infrared Spectro-radiometer, which uses a Michelson-Morley interferometer design,
384 with the path differences generated by an oscillating yoke with a corner-cube reflector on each
385 arm. Wavelength calibration is accomplished using a He-Ne laser. Radiometric calibration is
386 achieved by using two blackbodies whose cavities are maintained at known temperatures at
387 each of which the field of view of the interferometer is directed sequentially before and after
388 scene measurements. It had a 25 mm diameter entrance aperture and a spectral resolution of
389 0.5 cm^{-1} . Its temperature resolution was quoted as 5 mK. The M-AERI Mk-3 had a field of
390 view of 2.58 degrees (full angle) and responded over the 3300 cm^{-1} to 525 cm^{-1} range ($3 \text{ }\mu\text{m}$ to
391 $19 \text{ }\mu\text{m}$ wavelength range). The brightness temperature of the ammonia heat-pipe blackbody
392 was provided at two wavenumbers, 1000 cm^{-1} ($10 \text{ }\mu\text{m}$) and 1302 cm^{-1} ($7.68 \text{ }\mu\text{m}$) with quoted
393 combined uncertainties of 18 mK and 40 mK respectively. Full information on this radiometer
394 can be found in Minnett et al., (2001).

395

396 **5 RESULTS AND DISCUSSION**

397

398 Figure 3 plots, as an example, the measurements provided by the STFC RAL SISTeR
399 radiometer (orange circles) when viewing the NPL blackbody maintained at about 10 °C and
400 the corresponding measurements of the cavity temperature made by the NPL (blue dashes).
401 Similar plots corresponding to all participating radiometers and for all ammonia heat-pipe
402 blackbody temperatures for which measurements were made can be found elsewhere (Barker
403 Snook, et al., 2017). Also plotted in the same figure are the combined uncertainty values of the
404 measurements made by SISTeR (orange error bars) and those of the NPL blackbody
405 measurements (blue error bars). From the measurements shown in Figure 3, the difference
406 between the average of the measurements made by the SISTeR radiometer over this time period
407 and the average of the corresponding NPL measurements of the blackbody temperature was
408 estimated to be 60 mK.

409 Figures 4 to 10 show the plots of the mean of the differences between the radiometer readings
410 and the corresponding NPL measurements of the temperature of the ammonia heat-pipe
411 reference blackbody, for all the blackbody temperatures at which the radiometers were
412 compared. The uncertainty bars shown in these Figures represent the combined standard
413 uncertainty ($k = 1$) of the measurements provided by the participants and includes the
414 uncertainty contribution due to the ammonia heat-pipe blackbody.

415 It is clear that the uncertainty of measurements reported by radiometers which included internal
416 blackbodies for continuous calibration of their responsivity is significantly lower than the
417 corresponding uncertainty of radiometers which did not include internal references. This was
418 to be expected because the responsivity of infrared detectors is known to drift due to a number
419 of reasons (see for example, Theocharous and Theocharous, 2006). The use of internal
420 references such as the blackbodies included within the radiometers allowed the effects of these
421 drifts to be arrested, thus reducing the combined uncertainty of their measurements. This is
422 also reflected in the difference between the measurements made by these radiometers and the

423 temperature of the ammonia heat pipe blackbody. Measurements made by radiometers with
424 internal blackbodies generally provided better agreement compared to measurements reported
425 by radiometers which did not have internal references.

426 Examination of Figures 4 to 10 indicate that some cases exist in which the measurements
427 reported by the ammonia heat-pipe blackbody were well outside the uncertainty bars of
428 measurements reported by participating radiometers, even radiometers which included internal
429 reference blackbodies. A major part of this discrepancy can be explained on the basis that the
430 uncertainty bars shown in Figures 4 to 10 represent the one-sigma ($k=1$) uncertainty values. If
431 the uncertainty bars were extended to represent the three-sigma ($k=3$) case, then the uncertainty
432 bars of all measurements reported by radiometers which included internal reference
433 blackbodies would have included the corresponding measurements reported by the ammonia
434 heat-pipe blackbody.

435 Figures 4 to 10 show that the differences between the participants' radiometer readings and the
436 corresponding temperature of the NPL reference blackbody became progressively larger,
437 particularly as the reference blackbody temperature decreased to $-15\text{ }^{\circ}\text{C}$ and $-30\text{ }^{\circ}\text{C}$. This
438 observation is not altogether surprising because measurements were made in a lab, with the
439 measuring radiometers operating at ambient temperatures. This means that the internal
440 blackbodies within the participating radiometers (which provided the reference against which
441 the radiometers were basing their measurements) were also operating at near ambient
442 temperatures; hence for low temperatures of the ammonia heat-pipe blackbody, the difference
443 between the temperature of the test blackbody and the internal reference blackbodies increased,
444 probably leading to the observed discrepancies. The discrepancies are likely to arise due to the
445 large extrapolation ranges (up to $50\text{ }^{\circ}\text{C}$) and may be enhanced by other effects. If, for example,
446 the out-of-band response of a radiometer was measured incorrectly or had a small undetected
447 spectral leak, then discrepancies are likely to arise. It is estimated that the output of a radiometer

448 responding in the 10 μm to 11 μm region, which is calibrated at 30 $^{\circ}\text{C}$ and extrapolated to -
449 30 $^{\circ}\text{C}$, will be 0.26 % different from the output obtained if the radiometer had an out-of-band
450 response in the 5 μm to 6 μm region which was just 1 % of the response in the 10 μm to 11 μm
451 band.

452 It is important to point out that if the radiometers were used to measure low temperature targets,
453 such as the surface temperature of ice in the arctic, then the radiometers (as well as the internal
454 blackbodies) will also be at low temperatures so the extrapolation will not be over a significant
455 temperature range. This means that the discrepancies between the radiometer measurement of
456 the ice and the true surface temperature of ice are likely to be much smaller. For future
457 comparisons where such low temperatures are important, consideration should be given to how
458 the ambient temperature of the radiometers can be reduced to be more representative of the
459 operational environment.

460 Moreover, as the temperature of the reference blackbody decreases, the signal detected by the
461 photodetectors within the radiometers also decreases, resulting in poorer signal-to-noise ratios.
462 The poorer signal-to-noise ratios would result in measurements with poorer Type A uncertainty
463 and thus more unreliable measurements due to the resulting higher combined uncertainty.

464 It is important to note that the NPL AMBER radiometer was used in the past to measure the
465 temperature of the same ammonia heat-pipe reference blackbody used in this comparison and
466 the agreement between the NPL AMBER measurements and the blackbody measurements was
467 good, indicating its reliability. In fact the difference between the NPL AMBER measurements
468 and the reference blackbody measurements are included in the Figures for blackbody
469 temperatures of -30 $^{\circ}\text{C}$, 0 $^{\circ}\text{C}$, 10 $^{\circ}\text{C}$, 20 $^{\circ}\text{C}$ and 30 $^{\circ}\text{C}$. The agreement between the AMBER and
470 the reference blackbody measurements indicates that the discrepancies observed in the
471 measurements of some radiometers (which can be as large as 2 K for blackbody temperatures

472 around -30 °C) do not arise due to issues with the blackbody but are likely to be associated with
473 the participants' measurements. Furthermore, NPL AMBER radiometer was used to measure
474 the temperature of the ammonia heat-pipe blackbody of PTB, the German national standards
475 lab, and that comparison also showed good agreement between the measurements provided by
476 NPL AMBER and those provided by the PTB reference blackbody, as shown in Figure 4 in the
477 paper by Gutschwager (Gutschwager et al., 2013) which deals with that comparison.

478 The NPL reference blackbody had an aperture of 75 mm in diameter which could be decreased
479 by adding apertures with diameters smaller than 75 mm on the blackbody casing (see Figure 1).
480 The distance between the front of the blackbody cavity and the aperture formed/mounted on
481 the blackbody casing was also 75 mm, meaning that the Field of View (FoV) of a radiometer
482 placed against the casing would be overfilled by the blackbody cavity, provided its half angle
483 was less than 26.5° (53° full angle). Although the 75 mm diameter of the blackbody and its
484 position were defined and open for review in the protocol before the measurements took place,
485 this could be a source of error for radiometers with a large angle field of view (e.g. the ONERA
486 MR354SC, IR120, SISTeR and CE312-2 radiometers), as well as radiometers which could not
487 be positioned close to the blackbody casing aperture (e.g. M-AERI Mk-3). For these
488 radiometers, the measurements taken would likely capture the edges of the blackbody cavity,
489 as well as radiation emitted by blackbody cavity, thus introducing biases to the measurements.
490 To avoid this problem, some participants made their measurements with their radiometers as
491 close to the blackbody front aperture as possible. Although this was considered to be a
492 satisfactory compromise, care should be taken because the emissivity of the NPL reference
493 blackbody is not unity. This meant that when a test radiometer was brought very close to the
494 blackbody aperture it partly “saw itself” reflected by the blackbody because the blackbody is
495 no longer exposed to ambient temperature but the temperature of the radiometer. This is a
496 particular problem with radiometers which operate at cryogenic temperatures.

497 For the temperatures below 0 °C, ice began to form near the aperture of the reference blackbody
498 cavity. While the ice only formed near the entrance to the cavity (the cavity was continuously
499 purged with dry nitrogen gas), the presence of the ice may have affected the effective emissivity
500 of the areas of the blackbody cavity on which ice was deposited and thus alter the effective
501 emissivity of the reference blackbody for radiometers with very large FoVs. This may also
502 have impacted some of the results associated with the measurement of the temperature of
503 blackbody cavity. However, the same measurements were made using the NPL AMBER
504 radiometer and no discrepancies were observed for blackbody temperatures as low as -45 °C,
505 indicating that no ice was formed inside the reference blackbody cavity.

506 For the majority of radiometers being compared, their intended use was for sea surface
507 temperature measurements. For this reason, the majority of the participants used blackbodies
508 to calibrate their radiometers which could not operate below 0 °C, while some participants used
509 blackbodies which could not operate below ambient temperature. This meant that the
510 temperature range over which the majority of radiometers were calibrated was for temperatures
511 above 0 °C and in some cases temperatures above ambient. This means that some
512 measurements taken during this laboratory comparison were outside the range of calibrated
513 temperatures for these instruments so measurements made at the lower temperatures relied on
514 the extrapolation of the calibrations at higher temperatures. Any consideration of irregularities
515 with the values for measurements and their associated uncertainties made below 0 °C should
516 take this into account.

517 During the 2016 radiometer comparison, a 30 minute period was allocated to each participant
518 to allow for the alignment of the radiometer to the reference blackbody aperture and the making
519 of the measurements at a particular blackbody temperature. Some participants reported that
520 30 minutes was not enough. However, because of the number of radiometers participating in
521 the 2016 comparison and the number of temperatures which had to be completed over the

522 week-long comparison, the 30 minute period could not be extended. It is recommended that in
523 future comparisons, participants should be asked to state how long they would ideally require
524 in order to align and complete a measurement (at a particular blackbody temperature). If the
525 total duration of the comparison could not be extended, or the number of participating
526 radiometers could not be reduced, then the number of reference blackbody temperatures at
527 which measurements are done should be reduced to allow participants the extra time periods
528 they require to complete their measurements.

529

530 **6 CONCLUSIONS**

531

532 The performance of a number of radiometers was compared in the lab by measuring the
533 brightness temperature of the NPL ammonia heat-pipe blackbody at a number of temperatures
534 in the -30 °C to +45 °C temperature range. The results show that measurements of the reference
535 blackbody for cavity temperatures above 0 °C reported by radiometers which include internal
536 blackbodies exhibit superior measurement uncertainties and provide better agreement with
537 measurements reported by the ammonia heat-pipe blackbody compared to radiometers which
538 rely on infrequent re-calibration using external blackbodies. Furthermore, although the
539 Figures indicate that some cases exists in which the measurements reported by the ammonia
540 heat-pipe blackbody were well outside the uncertainty bars of measurements reported by
541 participating radiometers (even radiometers which included internal reference blackbodies),
542 this can be explained on the basis that the uncertainty bars shown in the Figures represent the
543 one-sigma ($k=1$) uncertainty values. If the uncertainty bars were extended to represent the
544 three-sigma ($k=3$) case, then the uncertainty bars of all measurements reported by radiometers
545 which included internal reference blackbodies would have included the corresponding
546 measurements reported by the ammonia heat-pipe blackbody.

547 Participants were encouraged to provide detail uncertainty budgets for all measurements they
548 provided. Although uncertainty estimates were provided by all participants for all
549 measurements they reported as part of the 2016 comparison, the level of detail which was
550 included in the uncertainty budgets varied significantly from one participant to the next, with
551 some participants providing only a value for the estimate of the uncertainty of their
552 measurements. It is recommended that participation in future comparisons should be made
553 conditional on participants providing full uncertainty budgets for all measurements they
554 provide as part of the comparison activity.

555 The 2016 comparison showed that the differences between the readings of the participating
556 radiometer and the corresponding temperature of the reference blackbody increased,
557 particularly for measurements corresponding to reference blackbody temperatures below 0 °C.
558 Reasons for the discrepancies observed at low blackbody temperatures were put forward,
559 including the extrapolation from the calibration of the radiometers using blackbodies operating
560 at ambient temperatures, combined with the absence of any information on the relative spectral
561 responsivity of the radiometers. These discrepancies are not expected to arise, if the
562 radiometers were calibrated with a reference blackbody operating at these low temperatures.
563 Furthermore, any discrepancies which were measured at low blackbody temperatures may be
564 considered irrelevant because the majority of the radiometers taking part in this comparison
565 will be used to measure sea surface temperature i.e. temperatures above 0 °C.

566

567 **7 ACKNOWLEDGEMENTS**

568

569 The authors wish to thank Miss Helen McEvoy and Mr Jamie McMillan (both of NPL) for their
570 assistance in operating the ammonia heat-pipe blackbody and with the testing surrounding the
571 radiometer laboratory comparison. The authors also wish to thank ESA for funding this work

572 under ESA Contract No: 4000113848_15I-LG. The University of Valencia participation in the
573 2016 FRM4STS comparison was funded by the Spanish Ministerio de Economía y
574 Competitividad and the European Regional Development Fund (FEDER) through the project
575 CGL2015-64268-R (MINECO/FEDER, UE) and by the Ministerio de Economía y
576 Competitividad through the project CGL2013-46862-C2-1-P (MINECO). The Ocean
577 University of China participation in the 2016 FRM4STS comparison was funded by the
578 National Natural Science Foundation of China under Grant 41376105 and the Global Change
579 Research Program of China under Grant 2015CB953901. The Universidad de La Laguna
580 participation was supported by Spanish Ministerio de Economía y Competitividad under
581 project CGL2013-48202-C2-1-R.

582

583 **8 REFERENCES**

584 Barker Snook, I., E. Theocharous and N. P. Fox, 2017: 2016 comparison of IR brightness
585 temperature measurements in support of satellite validation. Part 2: Laboratory comparison of
586 radiation thermometers. *NPL Report ENV 14*, 118 pp. see link [http://www.frm4sts.org/wp-](http://www.frm4sts.org/wp-content/uploads/sites/3/2017/12/FRM4STS_D100_TR-2_Part2_Radiometer_23Jun17-signed.pdf)
587 [content/uploads/sites/3/2017/12/FRM4STS_D100_TR-2_Part2_Radiometer_23Jun17-signed.pdf](http://www.frm4sts.org/wp-content/uploads/sites/3/2017/12/FRM4STS_D100_TR-2_Part2_Radiometer_23Jun17-signed.pdf)

588 Barton, I. J., P. J. Minnett, K. A. Maillet, C. J. Donlon, S. J. Hook, A. T. Jessup and T. J.
589 Nightingale, 2004: The Miami 2001 infrared radiometer calibration and intercomparison: Part
590 II Shipboard results. *J. Atmos. Oceanic Technol.*, **21**, 268-283.

591 Berry, K., 1981: Emissivity of a cylindrical black-body cavity with a re-entrant cone end face.
592 *J. Phys. E: Sci. Instrum.* **4**, 629–632.

593 Betts D. B., F. J. J. Clarke, L. J. Cox and J. A. Larkin, 1985: Infrared reflection properties of
594 five types of black coating for radiometric detectors. *J. Phys. E: Sci. Instrum.*, **18**, 689–696.

595 Chu, B and G. Machin, 1999: A low-temperature blackbody reference source to -40 °C.
596 *Meas. Science Technol.*, **10**, 1–6.

597 Donlon, C., I. S. Robinson, W. Wimmer, G. Fisher, M. Reynolds, R. Edwards and T. J.
598 Nightingale, 2008: An infrared sea surface temperature autonomous radiometer (ISAR) for
599 deployment aboard volunteer observing ships (VOS). *J. Atmos. Oceanic Technol.*, **25**, 93-113.

600 Gutschwager, B., E. Theocharous, C. Monte, A. Adibekyan, M. Reiniger, N. P. Fox and J.
601 Hollandt, 2013: Comparison of the radiation temperature scales of the PTB and the NPL in the
602 temperature range from -57 °C to 50 °C. *Meas. Science Technol.*, **24**, Article No 095002.

603 Legrand, M., C. Pietras, G. Brogniez, M. Haeffelin, N. K. Abuhassan. And M. Sicard, 2000: A
604 high-accuracy multiwavelength radiometer for in situ measurements in the thermal infrared.
605 Part I: characterization of the instrument, *J. Atmos. Ocean Technol.*, **17**, 1203-1214.

606 Minnett, P. J., R. O. Knuteson, F. A. Best, B. J. Osborne, J. A. Hanafin and O. B Brown, 2001:
607 The Marine-Atmosphere Emitted Radiance Interferometer (M-AERI), a high accuracy, sea-
608 going infrared spectroradiometer. *J. Atmos. Oceanic Technol.*, **18**, 994-1013.

609 Minnett, P. J., C. Gentemann, T. J. Nightingale, I. J. Barton, B Ward, B and M. J. Murray,
610 2002: Toward improved validation of satellite sea surface skin temperature measurements for
611 climate research. *J. Climate*, **15**, 353-369.

612 Minnett, P.J. and G. K. Corlett, 2012: A pathway to generating Climate Data Records of sea-
613 surface temperature from satellite measurements. *Deep Sea Research Part II: Topical Studies*
614 *in Oceanography*, **77–80**, 44-51

615 Rice, J. P., J. I. Butler, B. C. Johnson, P. J. Minnett, K. A. Maillet, T. J. Nightingale, S. J. Hook,
616 A. Abtahi, C. J. Donlon and I. J. Barton, 2004: The Miami 2001 infrared radiometer calibration

617 and intercomparison. Part I: Laboratory characterisation of blackbody targets. *J. Atmos.*
618 *Oceanic Technol.*, **21**, 258-267.

619 Sicard, M., P. R. Spyak, G. Brogniez, M. Legrand, N. K. Abuhassan, C. Pietras and J. P. Buis,
620 1999: Thermal infrared field radiometer for vicarious cross-calibration: characterization and
621 comparisons with other field instruments. *Opt. Engin.*, **38**, 345-356.

622 Theocharous, E., N. P. Fox, V. I. Sapritsky, S. N. Mekhontsev and S. P. Morozova, 1998:
623 Absolute measurements of black-body emitted radiance *Metrologia*, **35**, 549-554.

624 Theocharous, E. and Theocharous, O. J., 2006: Practical limit of the accuracy of radiometric
625 measurements using HgCdTe detectors *Applied Optics*, **45**, 7753-7759 Theocharous, E., E.
626 Usadi and N. P. Fox, 2010: CEOS comparison of IR brightness temperature measurements in
627 support of satellite validation. Part I: Laboratory and ocean surface temperature comparison of
628 radiation thermometers”, *NPL Report COM OP3*, 130 pp.

629 Theocharous, E. and N. P. Fox, 2010: CEOS comparison of IR brightness temperature
630 measurements in support of satellite validation. Part II: Laboratory comparison of the
631 brightness temperature of blackbodies. *NPL Report COM OP4*, 43 pp.

632 Wimmer, W., and I. Robinson, 2016: The ISAR instrument uncertainty model. *J. Atmos.*
633 *Oceanic Technol.*, **33**, 2415-2433.

634 Yoder, J. A., K. S. Casey and M. D. Dowell, 2014: Ocean Climate and satellite optical
635 radiometry, *Optical radiometry for Ocean climate measurements*, edited by G. Zibori, G. J.
636 Donlon and A.C. Parr, Published by Academic press, 3-12.

637

Table 1. Instruments involved in the 2016 CEOS infrared radiometers laboratory comparison.

| Radiometer | Institute | Waveband (μm) | Detector | Field of View ($^\circ$) | Reference |
|-------------------------|-----------------------|-------------------------------|------------------------|-------------------------------|---|
| CE312-2 (2 units) | UV ^a | 8.0 – 13.3 | Thermopile | 10 | Sicard et al. (1999) |
| KT15.85 IIP | KIT ^b | 9.6 – 11.5 | Pyroelectric | 8.3 | https://www.heitronics.com/fileadmin/content/Prospekte/KT15IIP_e_V510.pdf |
| KT19.85 II (3 units) | ONERA ^c | 9.6 – 11.5 | Pyroelectric | 1.36 | https://www.heitronics.com/fileadmin/content/Prospekte/KT15IIP_e_V510.pdf |
| MR354SC | ONERA ^c | 3.0 – 13.0 | MCT Photoconductive | 20 | https://library.e.abb.com/public/654dfb800019d7168525712d00693379/4314%20MR304SC%20Spec.pdf |
| ISAR-5D | CSIRO ^d | 9.6 – 11.5 | Pyroelectric | 7 | Wimmer & Robinson, (2004) |
| SISTeR | STFC/RAL ^e | 10.8 | Pyroelectric | 13 | Barton et al., (2004) |
| ISAR-5D | NOC ^f | 9.6 – 11.5 | Pyroelectric | 7 | Wimmer and Robinson, (2016) |
| ISAR-5D | DMI ^g | 9.6 – 11.5 | Pyroelectric | 7 | Wimmer and Robinson, (2016) |
| IR120 | DMI ^g | 8.0 – 14.0 | Thermopile | 20 | www.campbellsci.eu/ir120 |
| ISAR-5C | OUC ^h | 9.6 – 11.5 | Pyroelectric | 7 | Wimmer and Robinson, (2016) |
| OUCFIRST | OUC ^h | 9.6 – 11.5 | Pyroelectric | 7 | |
| CE312-2 | GOTA/ULL ⁱ | 8.1 – 11.7 | Thermopile | 10 | Sicard et al. (1999) |
| M-AERI | RSMAS ^j | 3.0 – 18.0 | Cooled InSb and HgCdTe | 2.58 | Minnett et al., (2001) |

639

640 ^a University of Valencia (Spain)641 ^b Karlsruhe Institute of Technology (Germany)642 ^c Office National d'études et de Recherches Aéropatiales (France)643 ^d Commonwealth Scientific and Industrial Research Organisation (Australia)644 ^e Science and Technology Facilities Council Rutherford Appleton Laboratory (UK)645 ^f National Oceanography Centre (UK)646 ^g Danish Meteorological Institute (Denmark)647 ^h Ocean University of China (China)648 ⁱ Grupo de Observación de la Tierra y la Atmósfera/Universidad de La Laguna (Spain)649 ^j Rosenstiel School of Marine and Atmospheric Sciences (USA)

650

651

652 **Figure captions:**

653

654 Figure 1: Schematic of the ammonia heat-pipe blackbody.

655

656 Figure 2: The RASMAS M-AERI radiometer viewing the ammonia heat-pipe blackbody
657 during the 2016 radiometer comparison.

658

659 Figure 3: Measurements of the STFC RAL SISTeR radiometer viewing the NPL reference
660 blackbody maintained at approximately 10 °C (in orange) and the corresponding measurements
661 made by NPL of the blackbody temperature (in blue).

662

663 Figure 4: Plot of the mean of the differences of the radiometer readings from the temperature
664 of the NPL reference blackbody, maintained at a nominal temperature of -30 °C.

665

666 Figure 5: Plot of the mean of the differences of the radiometer readings from the temperature
667 of the NPL reference blackbody, maintained at a nominal temperature of -15 °C.

668

669 Figure 6: Plot of the mean of the differences of the radiometer readings from the temperature
670 of the NPL reference blackbody, maintained at a nominal temperature of 0 °C.

671

672 Figure 7: Plot of the mean of the differences of the radiometer readings from the temperature
673 of the NPL reference blackbody, maintained at a nominal temperature of 10 °C.

674

675 Figure 8: Plot of the mean of the differences of the radiometer readings from the temperature
676 of the NPL reference blackbody, maintained at a nominal temperature of 20 °C.

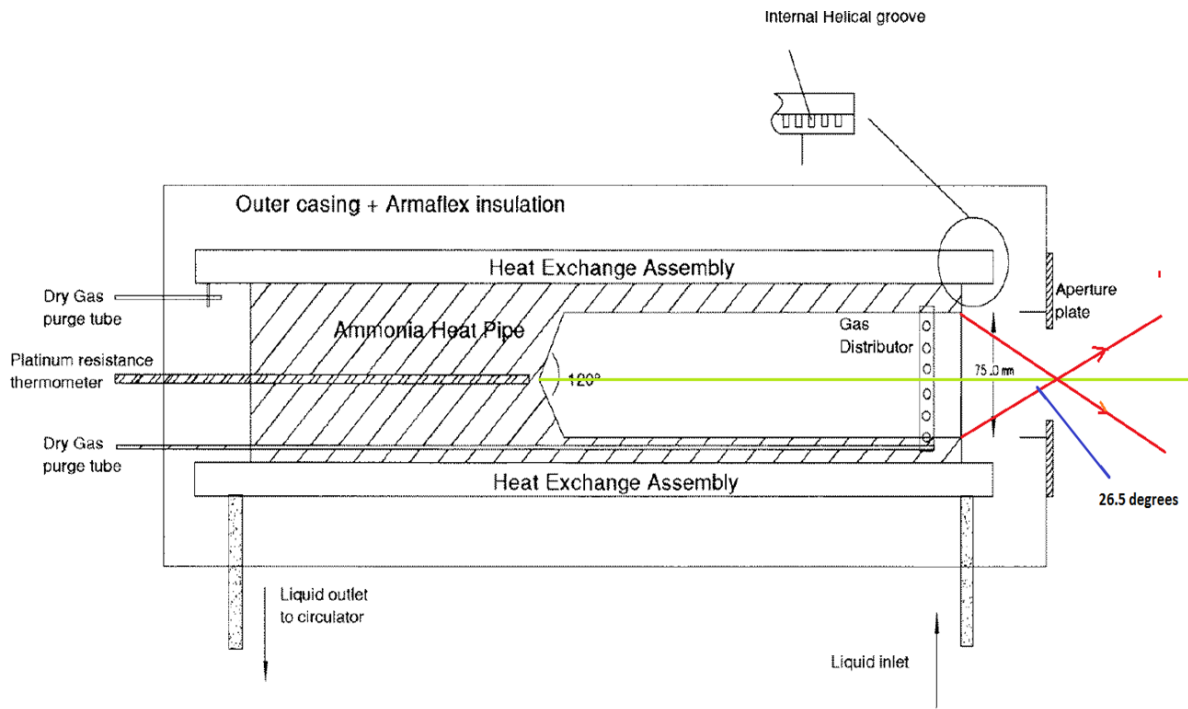
677

678 Figure 9: Plot of the mean of the differences of the radiometer readings from the temperature
679 of the NPL reference blackbody, maintained at a nominal temperature of 30 °C.

680

681 Figure 10: Plot of the mean of the differences of the radiometer readings from the temperature
682 of the NPL reference blackbody, maintained at a nominal temperature of 45 °C.

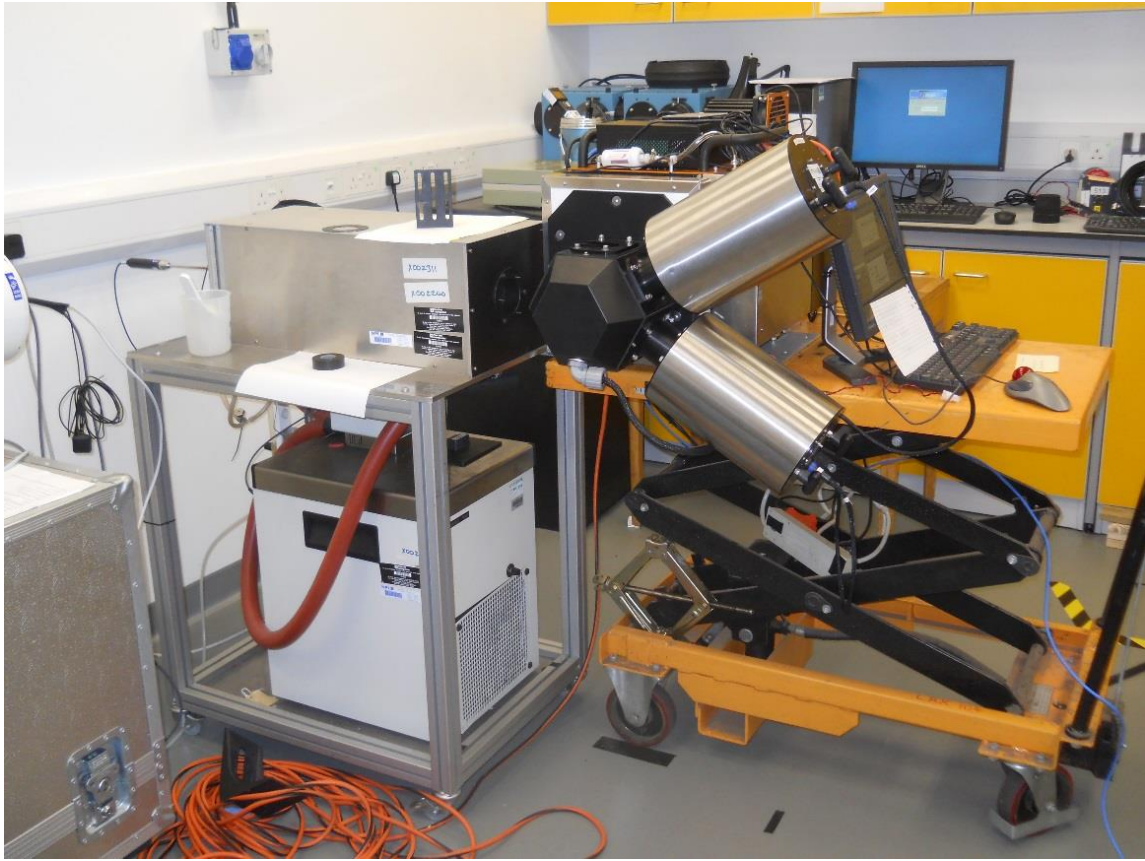
683



684

685

Figure 1: Schematic of the ammonia heat-pipe blackbody

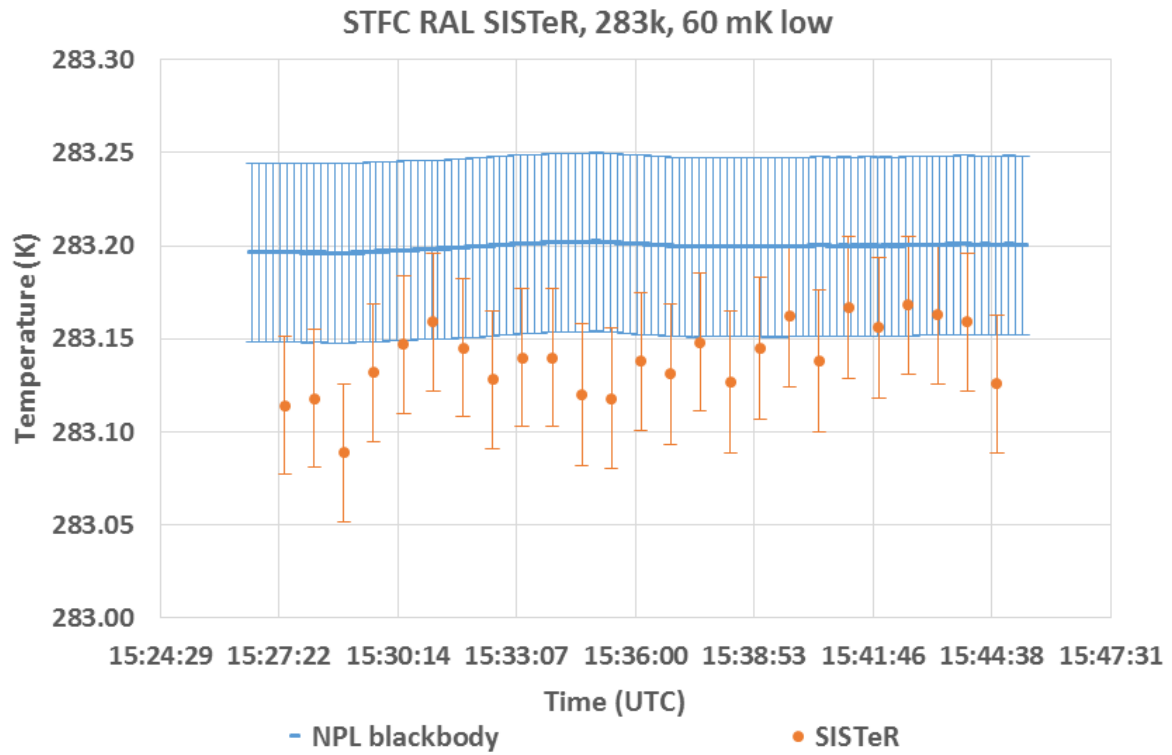


686

687

688 Figure 2: The RSMAS M-AERI radiometer viewing the ammonia heat-pipe blackbody during

689 the 2016 radiometer comparison.



690

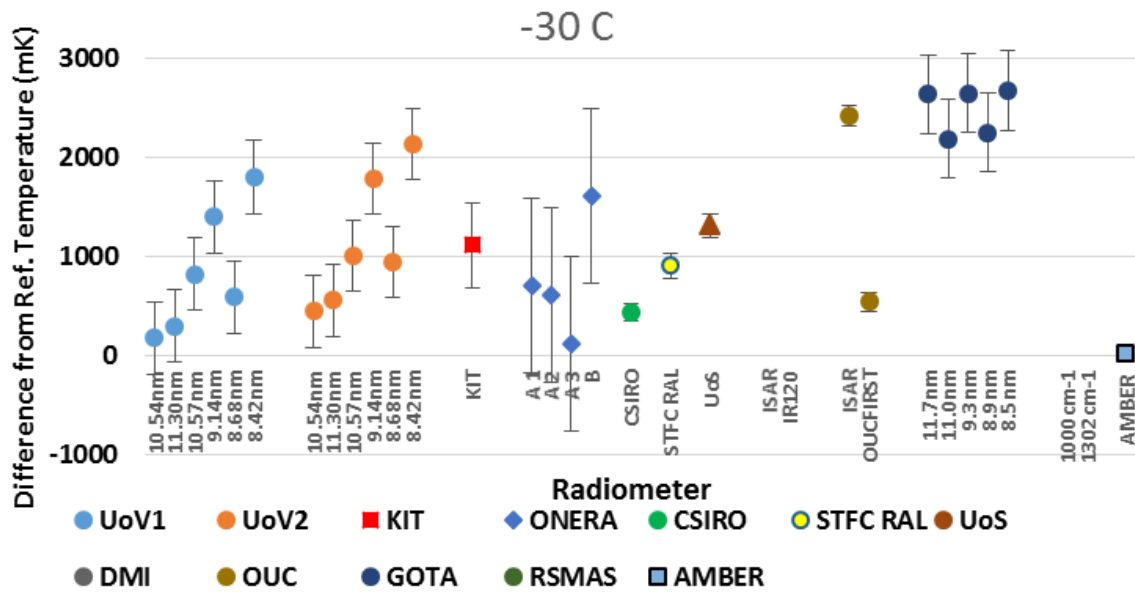
691

692 Figure 3: Measurements of the STFC RAL SISTeR radiometer viewing the NPL reference

693 blackbody maintained at approximately 10 °C (in orange) and the corresponding measurements

694 made by NPL of the blackbody temperature (in blue).

695

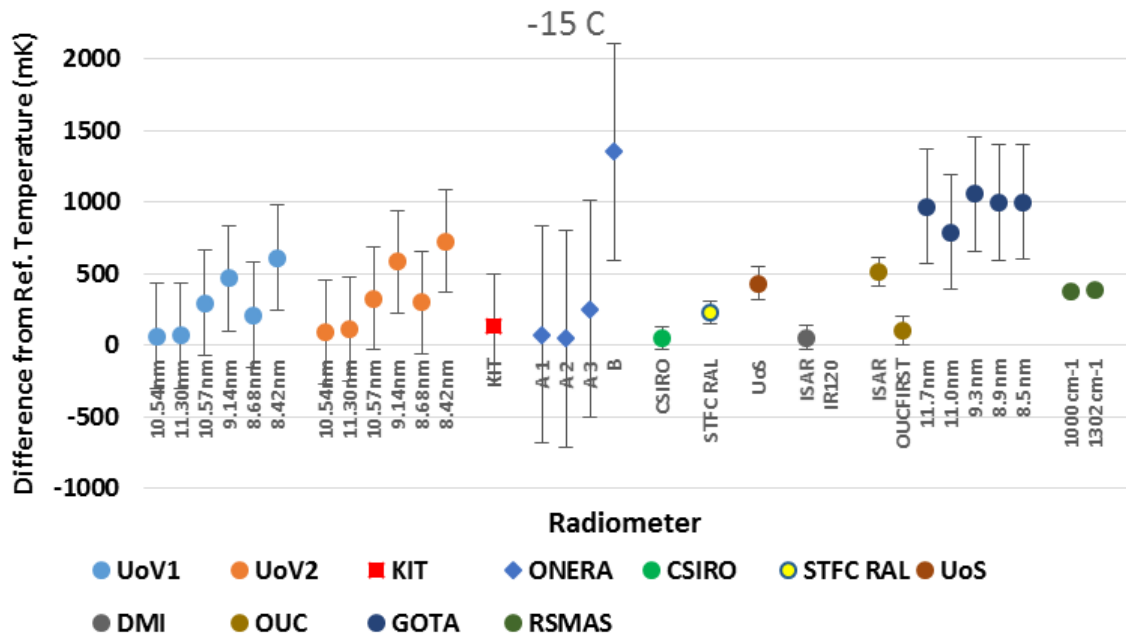


696

697

698 Figure 4: Plot of the mean of the differences of the radiometer readings from the temperature
699 of the NPL reference blackbody, maintained at a nominal temperature of -30 °C.

700



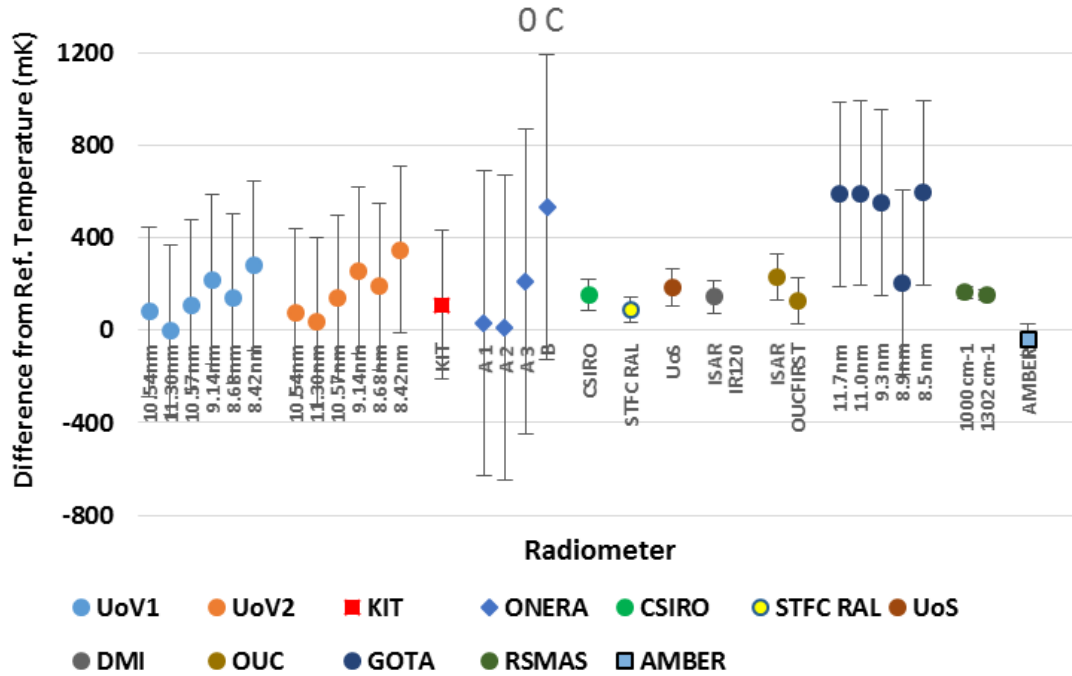
701

702

703 Figure 5: Plot of the mean of the differences of the radiometer readings from the temperature
704 of the NPL reference blackbody, maintained at a nominal temperature of -15 °C.

705

706



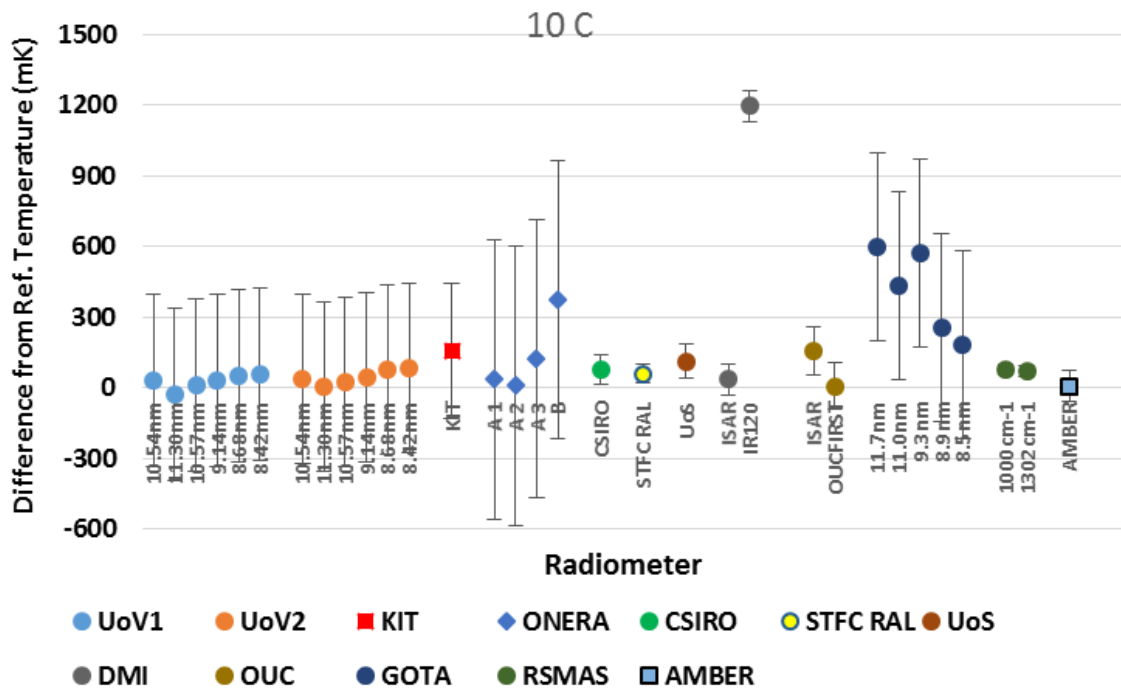
707

708

709 Figure 6: Plot of the mean of the differences of the radiometer readings from the temperature

710 of the NPL reference blackbody, maintained at a nominal temperature of 0 °C.

711

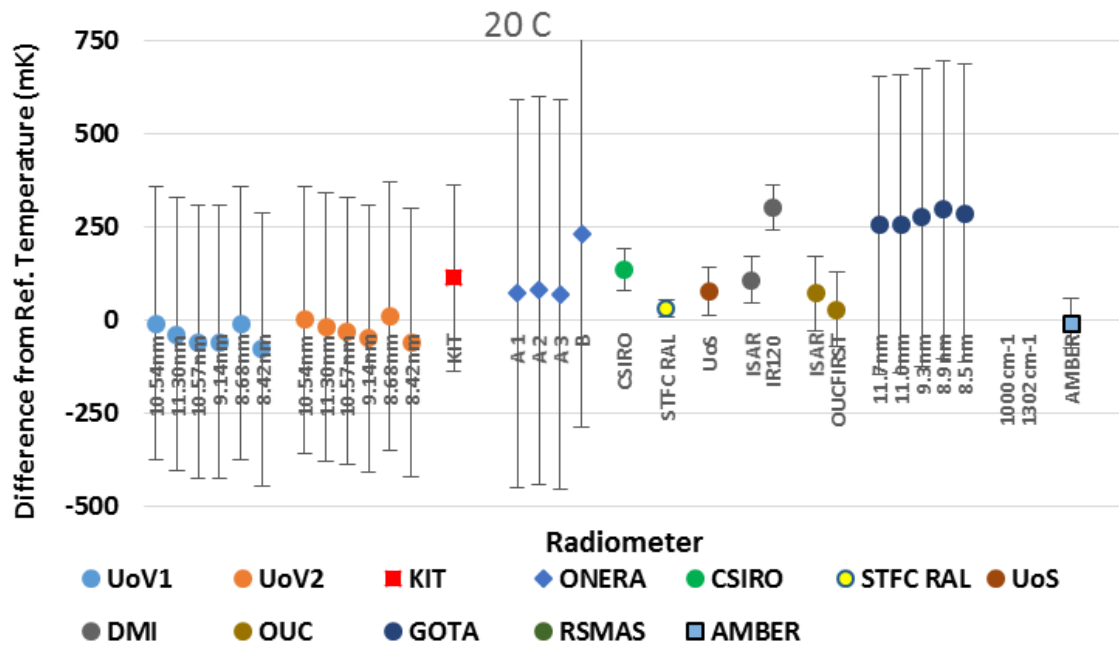


712

713

714 Figure 7: Plot of the mean of the differences of the radiometer readings from the temperature
715 of the NPL reference blackbody, maintained at a nominal temperature of 10 °C.

716



717

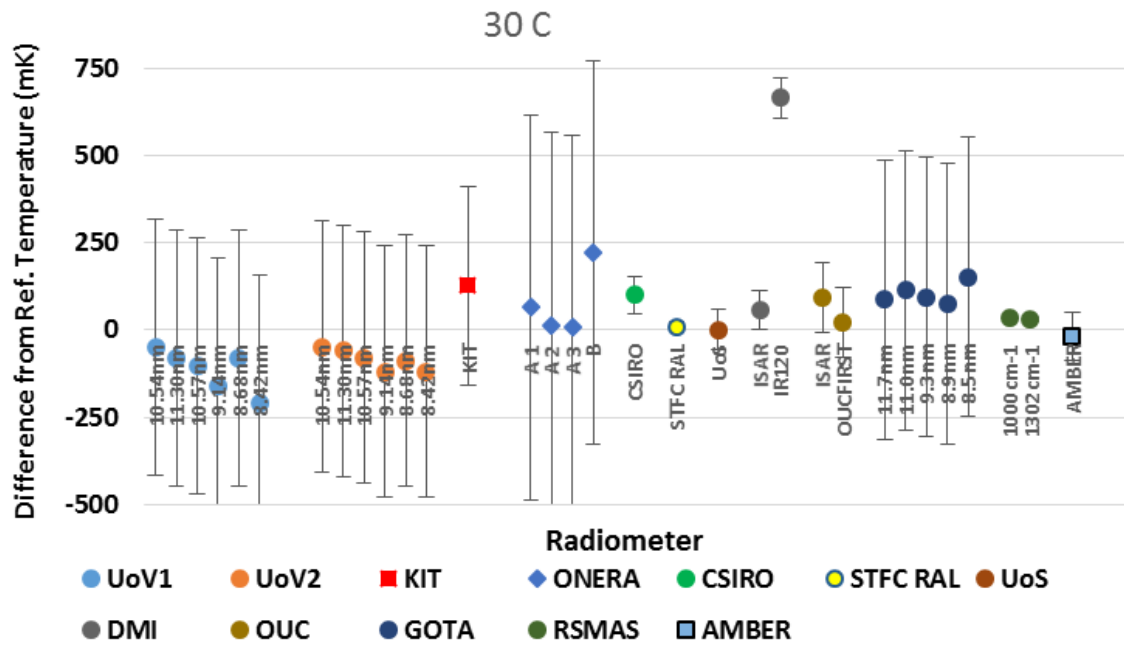
718

719 Figure 8: Plot of the mean of the differences of the radiometer readings from the temperature
720 of the NPL reference blackbody, maintained at a nominal temperature of 20 °C.

721

722

723



724

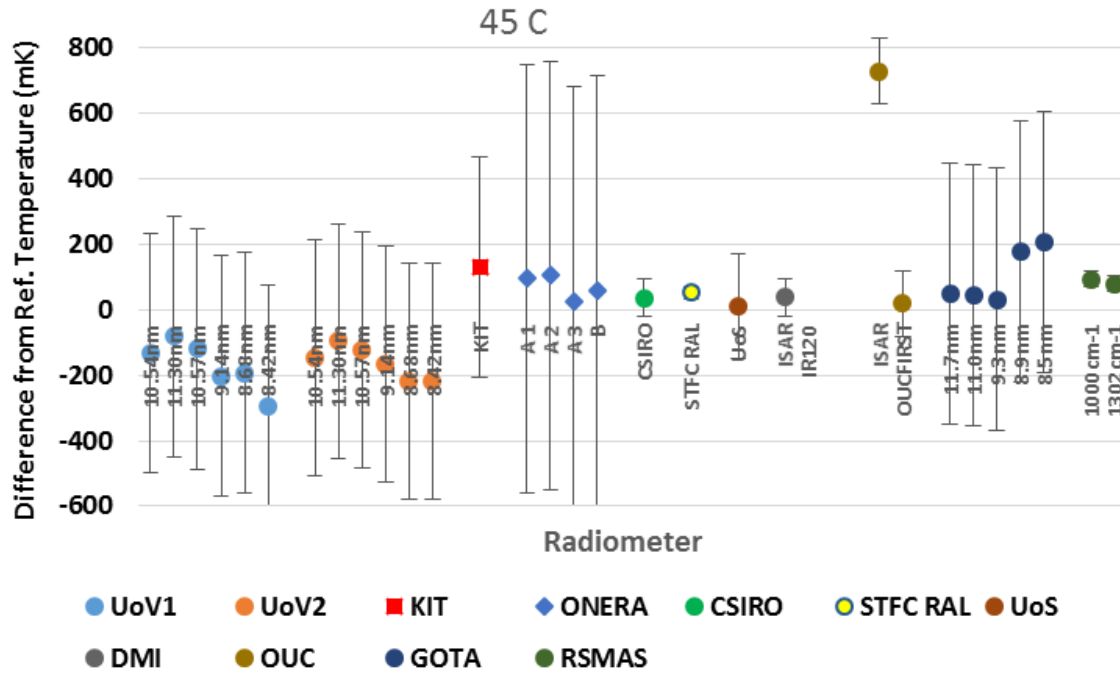
725

726 Figure 9: Plot of the mean of the differences of the radiometer readings from the temperature

727 of the NPL reference blackbody, maintained at a nominal temperature of 30 °C.

728

729



730

731 Figure 10: Plot of the mean of the differences of the radiometer readings from the temperature

732 of the NPL reference blackbody, maintained at a nominal temperature of 45 °C.